Failure Analysis of Reinforced Concrete Shell Structures using Layered Shell Element with Pressure Node

Ha-Wong Song, M.ASCE[1]; Sang-Hyo Shim[2]; Keun-Joo Byun, M.ASCE[3]; and Koichi Maekawa, M.ASCE[4]

Abstract: In this paper, a finite element analysis technique is presented for the path-dependent nonlinear failure analysis of reinforced concrete shell structures. A so-called pressure node is added into a layered shell element utilizing in-plane constitutive models of reinforced concrete and layered formulation in the failure analysis. By controlling the volume of the shell structures using the pressure node, postpeak softening behavior after the ultimate load of the shell structures is obtained. Since the constitutive models cover loading, unloading, and reloading paths, the element is capable of predicting the behaviors of reinforced concrete shells under cyclic loading. For verification of the techniques in this paper, failure analyses of reinforced concrete slabs subjected to in-plane and out-of-plane loads and cyclic transverse loads are performed and numerical results are compared with experimental data. In addition, reinforced concrete dome structures designed with different reinforcement ratios are also analyzed to check the applicability of the technique in this paper. Results show that the techniques can be applied effectively to the failure analysis of various types of reinforced concrete shell structures.

DOI: 10.1061/(ASCE)0733-9445(2002)128:5(655)

CE Database keywords: Failure investigation; Shell structures; Concrete, reinforced; Finite element method.

Introduction

Recently an increasing number of complex reinforced concrete (RC) shell structures, such as underground tanks, reactor containers, silos, and cooling towers have been built. The combination of three-dimensional geometrical complexity and the loading conditions of shell structures, as well as the three-dimensional nonlinear behaviors of RC make conventional analytical techniques insufficient to predict the behavior of the RC structures accurately. Considering that some of the structures are located in seismic zones and subjected to dynamic loads, the path-dependent three-dimensional nonlinear analysis of RC shell structures is indispensable for correct simulation of their behaviors under cyclic or reversed cyclic loads. New and more efficient analytical procedures are needed for this purpose. The nonlinear finite element analysis technique has become widely used to meet this demand. A lot of effort has gone into the development and application of finite element analysis techniques for reinforced concrete plates and shells. With worldwide research efforts on the finite element method, it can now be used to simulate the structural performance of complex reinforced concrete shell structures. Even though many of these works present efficient solution algorithms with attention to the implementation of realistic constitutive models that can accurately predict the behavior of concrete shells, no realistic constitutive models for reinforced concrete three-dimensional shells under cyclic loads have been provided. In addition, effective algorithms to overcome instability in the post-peak failure behavior of the shell structures are limited.

The accuracy of the analytical technique for RC shell structures depends mainly on its ability to predict the second-order effects that cause nonlinearities. The factors that cause nonlinearities in RC include tension stiffening, compression softening, and stress-transfer nonlinearities around cracks; these are usually accounted for in constitutive models of RC. Another source of nonlinearity is the geometry of structure, which is generally considered by the inclusion of a second-order term of strains. However, the inclusion of higher order terms of strains does not provide a remedy to overcome the structural instability of RC shell structures due to either buckling or sudden brittle failure of the reinforced shell structures. Since a standard method to include the effect of geometrical nonlinearity is readily available (Zienkiewicz and Taylor 1991), the main factor affecting the level of analytical accuracy remains in the constitutive models installed inside the finite element program and a solution algorithm to overcome the instability.

In order to develop a generic, path-dependent, three-dimensional reinforced concrete shell element, two-dimensional constitutive equations and a layered formulation are utilized. For the modeling of a shell structure, a multilayered shell element is adopted. Then, a set of constitutive models based on the averaged stress–strain fields of cracked concrete and reinforcement is applied to each layer of the shell element. These constitutive relationships comprise a model of cracked concrete in compression, incorporating compression-softening effects due to transverse cracking, a model of cracking concrete in tension, reflecting

[1]Professor, Dept. of Civil Engineering, Yonsei Univ., Seoul 120-749, Korea (corresponding author). E-mail: song@yonsei.ac.kr

[2]Graduate Research Assistant, Dept. of Civil Engineering, Yonsei Univ., Seoul 120-749, Korea. E-mail: shim@yonsei.ac.kr

[3]Professor, Dept. of Civil Engineering, Yonsei Univ., Seoul 120-749, Korea. E-mail: byun@yonsei.ac.kr

[4]Professor, Dept. of Civil Engineering, Univ. of Tokyo, Tokyo 113, Japan. E-mail: maekawa@concrete.t.u-tokyo.ac.jp

Note. Associate Editor: Marc I. Hoit. Discussion open until October 1, 2002. Separate discussions must be submitted for individual papers. To extend the closing date by one month, a written request must be filed with the ASCE Managing Editor. The manuscript for this paper was submitted for review and possible publication on January 23, 2001; approved on August 20, 2001 . This paper is part of the ***Journal of Structural Engineering***, Vol. 128, No. 5, May 1, 2002. ©ASCE, ISSN 0733-9445/2002/5-655–664/$8.00+$.50 per page.

tension-stiffening effects due to bond interactions with reinforcement, a model of cracked concrete in shear, reflecting the aggregate interlocking, and a model of reinforcement in reinforced concrete. The models cover loading, unloading, and reloading paths. A multidirectional fixed smeared crack modeling of concrete (Okamura and Maekawa 1991) is applied to consider path-dependent parameters and mobilization of both cracks. A smeared-crack modeling based on cracked concrete in-plane constitutive law under cyclic loads proposed by Maekawa et al. (1997) is utilized to deal with the two-way cracking which accompanies crack opening and closing under cyclic loads. A finite element program incorporating these constitutive models is used to predict concrete shell structures subjected to in-plane and out-of-plane loads and cyclic transverse loads. For the postpeak softening behavior of reinforced shell structures, the so-called pseudovolume control method, which can analyze postpeak behaviors of concrete shell structures, is developed by adding a pressure node on the shell elements. The so-called pressure node has a single degree of freedom, namely, the uniform change of pressure on finite element. The distinctive characteristic of this shell element equipped with a pressure node is its capability to simulate the behavior of reinforced concrete shell structures under cyclic loads even for the postpeak softening range. With the pressure node formulation, one can control the change in volume enclosed by the shell structures and determine the required change in load. Thus, the pseudovolume control method with a pressure node can overcome the instability problem of the conventional force-control method. The method also overcomes the difficulty of selecting a local characteristic point to control the local displacement which governs the global behavior of shell structures in the conventional displacement-control method. The validity of the proposed analytical technique is verified by comparing analysis results with experimental data. The need to include the effect of geometrical nonlinearity on thin shells subjected to in-plane and out-of-plane loads is also shown. In addition, applicability of the pseudovolume control method is shown by analyzing typical reinforced dome structures designed with a different amount of reinforcement.

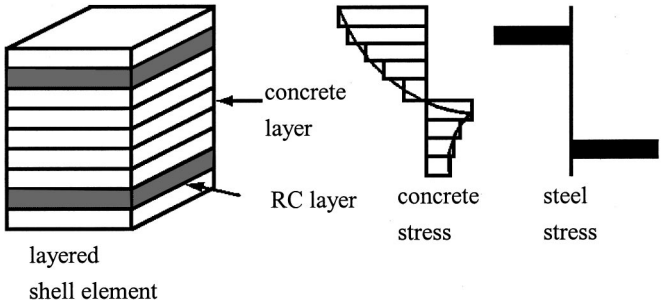

Fig. 1. Layered shell element

Formulation of Layered Shell Element

The element in this study is an isoparametric degenerated shell element (Worsak 1979) with six degrees of freedom in each node: three displacements (u, v, and w in x, y, and z directions) and three rotations ($\theta_x, \theta_y, \theta_z$ along x, y, and z axes), which are defined as **d**

$$\mathbf{d}=\{u,v,w,\theta_x,\theta_y,\theta_z\} \tag{1}$$

The last degree of freedom is in-plane rotation, sometimes referred to as the drilling degree of freedom (Hughes and Brezzi. 1989). By providing fictitious stiffness in this drilling degree of freedom ill conditioning, which may occur if all elements at a node are coplanar, is avoided. As the thickness of the shell decreases, the performance of the shell element is found to rapidly deteriorate (Zienkiewicz and Taylor 1991). In order to solve shear

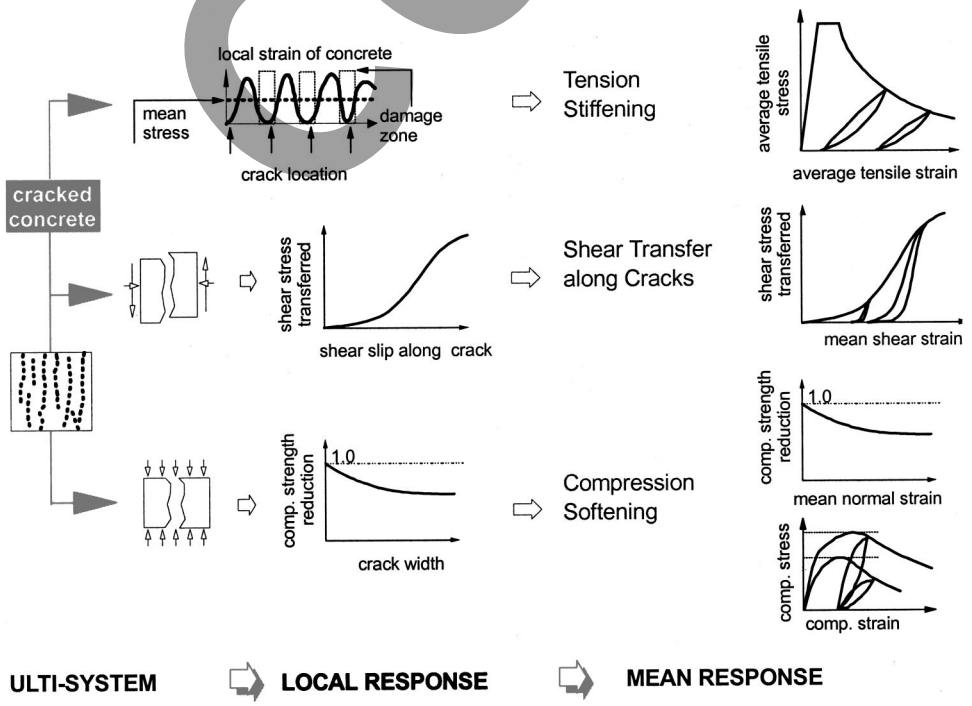

Fig. 2. In-plane constitutive models of cracked concrete

J. Struct. Eng., 2002, 128(5): 655-664

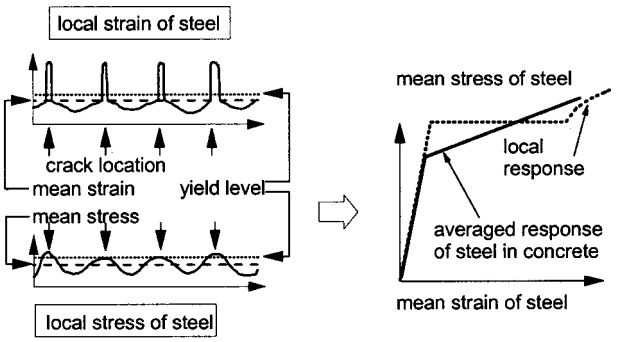

Fig. 3. Constitutive model of reinforcement embedded in concrete

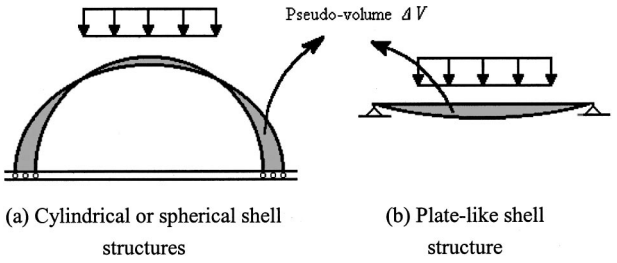

Fig. 5. Pseudovolume for shell structures

and membrane-locking problems associated with overconstraint of zero transverse shear strain and zero membrane strain conditions with an exact order of numerical integration for thin shells, a reduced order of numerical integration on Gaussian quadrature is used.

In the layered element formulation, the shell is divided into several layers where two-dimensional (2D) constitutive models are applied to take into account material nonlinearity. Each layer is classified as a steel layer and either plain concrete layer or reinforced concrete layer, where reinforcing bars are smeared in the layer, as shown in Fig. 1. Each layer of the layered shell element contains stress points on its midsurface. The stress components of the layer are computed at these stress points and are assumed to be constant over the thickness of each layer, so that the actual stress distribution of the shell is modeled by a piecewise constant approximation (see Fig. 1). A midpoint integration rule is applied for each layer.

A total Lagrangian formulation on Green–Lagrangian strain fields is applied to take into account the geometrical nonlinearity in the shell element where out-of-plane displacement w produces some additional extension in the in-plane displacement. In order to take into account shear deformation of the RC concrete shell, the Reissner–Mindlin formulation is adopted. Introducing the Von Karman assumptions, which imply that derivatives of in-plane displacements are small and noting that the variation of out-of-plane strain with thickness direction may be ignored, the generalized strain tensor, which is composed of Green–Lagrange strains of midsurface and curvatures, can be expressed as

$$\boldsymbol{\varepsilon}=\begin{Bmatrix}\overline{\varepsilon_x}\\ \overline{\varepsilon_y}\\ \overline{\gamma_{xy}}\\ \overline{\phi_x}\\ \overline{\phi_y}\\ \overline{\phi_{xy}}\end{Bmatrix}=\begin{Bmatrix}\dfrac{\partial u}{\partial x}\\ \dfrac{\partial v}{\partial y}\\ \dfrac{\partial u}{\partial y}+\dfrac{\partial v}{\partial x}\\ \dfrac{\partial \theta_y}{\partial x}\\ -\dfrac{\partial \theta_x}{\partial y}\\ \dfrac{\partial \theta_y}{\partial y}-\dfrac{\partial \theta_x}{\partial x}\end{Bmatrix}+\begin{Bmatrix}\dfrac{1}{2}\left(\dfrac{\partial w}{\partial x}\right)^2\\ \dfrac{1}{2}\left(\dfrac{\partial w}{\partial y}\right)^2\\ \dfrac{\partial w}{\partial x}\dfrac{\partial w}{\partial y}\\ 0\\ 0\\ 0\end{Bmatrix} \tag{2}$$

Then, in-plane strains in the xy plane in layer i can be written as

$$\varepsilon_x^i=\overline{\varepsilon_x}+z\overline{\phi_x}$$
$$\varepsilon_y^i=\overline{\varepsilon_y}+z\overline{\phi_y} \tag{3}$$
$$\gamma_{xy}^i=\overline{\gamma_{xy}}+z\overline{\phi_{xy}}$$

where z = distance from the midsurface of element thickness, and out-of-plane strains, such as transverse shear strain including shear deformation and rotation normal to the midsurface of the shell in the ith layer along the thickness of the element, can be written as

$$\gamma_{xz}^i=\frac{\partial w}{\partial x}+\theta_y$$

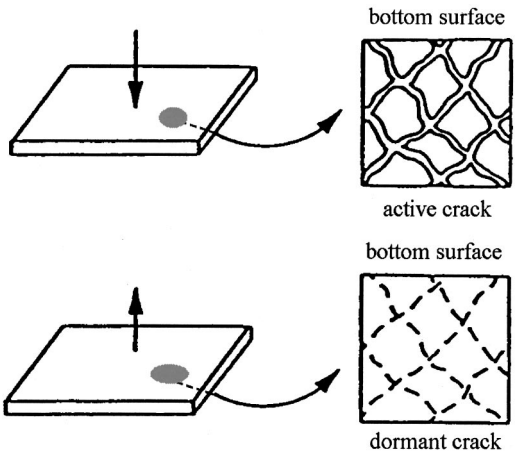

Fig. 4. Two-way active cracks in shell element under cyclic loads

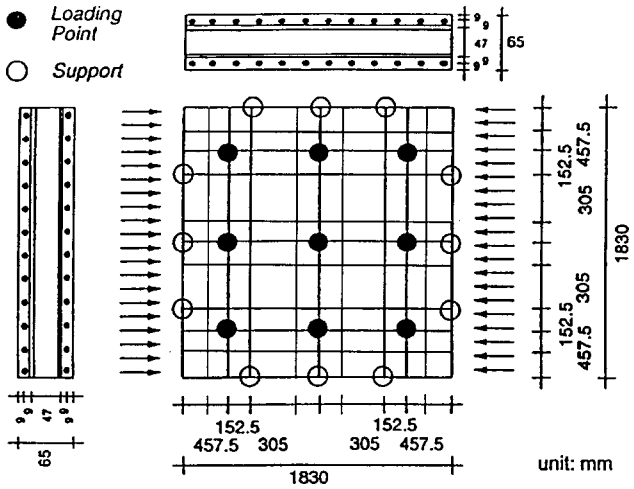

Fig. 6. Geometry and mesh used for specimen type A

J. Struct. Eng., 2002, 128(5): 655-664

$$\gamma_{yz}^{i}=\frac{\partial w}{\partial y}-\theta_x \tag{4}$$

$$\gamma_{zz}^{i}=\frac{1}{2}\left(\frac{\partial v}{\partial x}-\frac{\partial u}{\partial y}\right)-\theta_z$$

In-plane stresses in every layer can be obtained from in-plane strains in each layer through the utilization of in-plane constitutive models of reinforced concrete. Subsequently, in-plane internal forces such as membrane force and bending moments are calculated by integrating the corresponding stresses from each layer over the thickness of the element. Out-of-plane shear force and drilling force are obtained by multiplying the out-of-plane shear modulus of concrete and drilling stiffness to out-of-plane strains, respectively.

In matrix form, the generalized strain can be rewritten as

$$\boldsymbol{\varepsilon}=\mathbf{Bd}=[\mathbf{B}_L+\mathbf{B}_N]\mathbf{d} \tag{5}$$

where $\mathbf{B}_L$ contains the usual definition of strains, which is linear in displacement derivative, and $\mathbf{B}_N$=nonlinear portions. The discretized incremental equilibrium equation is derived by the principle of virtual work in its finite element total Lagrangian formulation, and can be written as

$$d\boldsymbol{\psi}=d\mathbf{R}-\int_V \mathbf{B}^T\, d\boldsymbol{\sigma}\, dV-\int_V d\mathbf{B}^T\, \boldsymbol{\sigma}\, dV \tag{6}$$

The first part of the right hand side of the equation represents the equivalent nodal force vector due to exterior loads, the second part represents normal stiffness matrix $\mathbf{K}_0$, and the third part represents the geometric stiffness matrix $\mathbf{K}_\sigma$. Since matrix **B** contains the nonlinear part, which depends on the displacement, it should be updated in each iteration. The solution to the nonlinear equilibrium equations is obtained by the Newton–Raphson method.

Constitutive Law of Reinforced Concrete Shell

By neglecting the stress component normal to the thickness of the thin shell, it is possible to reduce the three-dimensional (3D) stress field developed in the shells. In this simplification, the 3D confinement effect on concrete is neglected since the free stress boundary can be set toward the thickness direction. The 2D, in-plane constitutive law for RC is specified in each layer and the layer integration scheme of the RC shell (Polak 1992) is adopted. Each layer is classified as a plain concrete layer or RC layer where reinforcing bars are smeared in the layer (see Fig. 1). Since a certain amount of cracked concrete surrounding a reinforcing bar contributes to the stiffness of the element, the whole volume of concrete is considered to contribute to the tension stiffness of the element so that there is some tension softening effect even inside the plain concrete layer. The constitutive laws adopted for cracked concrete are derived based on the spatial average stress and the spatial average strain of concrete defined in finite elements, and they are composed of a tension stiffening model (Shima et al. 1987), a compression model (Maekawa and Okamura 1983), and a shear transfer model (Li et al. 1989) along cracks (Fig. 2) as described in Okamura and Maekawa (1991). By combining them with the model (Kato 1979) for reinforcing bars embedded in concrete (Fig. 3), the present model for a reinforced concrete shell element has been constructed. By using the averaged stress–strain relationships, the consistency and uniqueness of a constitutive law independent of size of crack spacing, crack density, and rebar diameter can be obtained. Prior to cracking, RC is modeled as elasto–plastic and a fracture material (Okamura and Maekawa 1991).

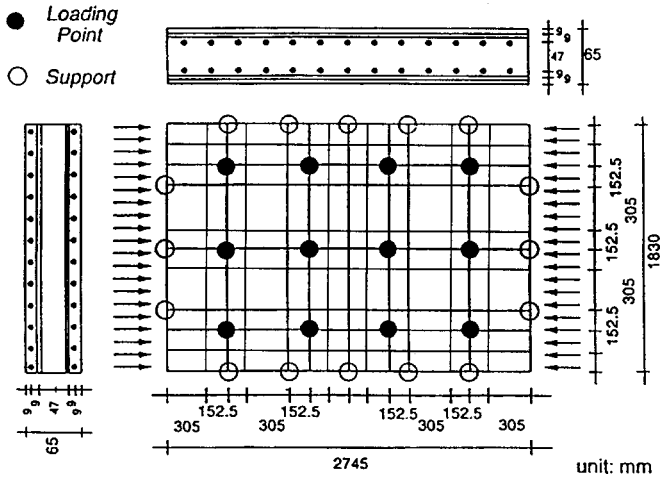

Fig. 7. Geometry and mesh used for specimen type B

Based on the multiple smeared, fixed crack concepts (e.g., de Borst and Nauta 1985), the smeared crack model with in-plane, two-way cracks (Okamura and Maekawa 1991) is used for the cracked concrete. Under out-of-plane loading, two sets of primary and secondary cracks might occur simultaneously. When the load is released, the two sets of cracks will close. The reversed cyclic load might create another two sets of primary and secondary cracks at a different layer along the thickness of the element. When the load is reversed again, the first two sets of cracks will open while the second sets of cracks will close. Fig. 4 illustrates the two-way active crack configuration in the shell element under cyclic loading conditions. The two-way active cracks observed in the shell element were found to govern overall nonlinear behaviors (Maekawa et al. 1997). Out-of-plane shear may occur peripherally when a concentrated load is set on RC shells.

Table 1. University of Alberta's Slab Specimens (Aghayere and MacGregor 1990)

Specimen	Concrete properties		Reinforcement			In-plane load (kN/m)
	f_c' (MPa)	E_c (MPa)	ρ_x (%)[a]	ρ_y (%)[a]	f_{sy} (MPa)	
A1	32.3	22,970	0.336	0.390	504	962
A2	32.3	23,010	0.350	0.400	504	765
B1	40.3	25,580	0.500	0.590	504	874
B2	40.2	25,550	0.500	0.590	504	634

Note: f_c': uniaxial compressive strength of concrete, E_c: elastic modulus of concrete, ρ_x, ρ_y: reinforcement ratio in x and y directions, and f_{sy}: yield stress of reinforcing bar.

[a]Per layer.

J. Struct. Eng., 2002, 128(5): 655-664

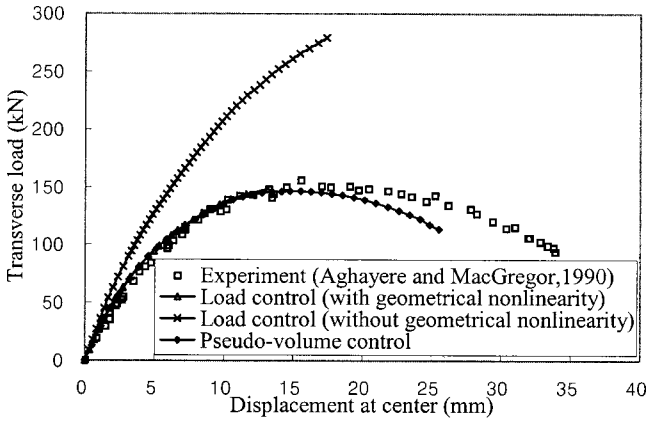

Fig. 8. Response of specimen A1

In a shell element, due to the possibility of two sets of cracks being active simultaneously, the loading condition of external loads to the specimen when each set of cracks occurs is recorded. A major crack is determined by comparing the crack width of the primary and secondary cracks. Cracks with a larger crack width are designated as major cracks. For minor cracks, the crack width and corresponding tension stress are compared to its previous maximum value at each loading step and updated if the present value is higher than the previous one. The corresponding tension stress of minor cracks is obtained from the tension stiffening model of reinforced concrete.

Pseudovolume Control Technique

Pseudovolume of Shell Element

Shell structures subject to external loads have deformed configuration compared to the original. A so-called pseudovolume of a shell element can be defined as the difference between a volume by original configuration and volume by deformed configuration changed by the corresponding external load (see Fig. 5). The original volume of a shell surrounded by boundary b can be defined as

$$V=\int_b \mathbf{n}^T\cdot\mathbf{x}\,db \tag{7}$$

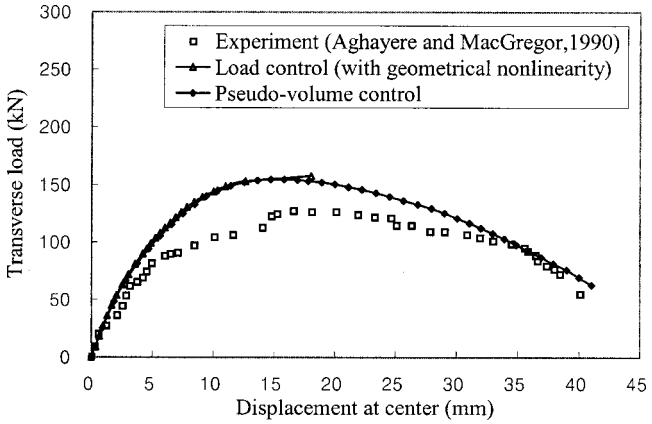

Fig. 9. Response of specimen A2

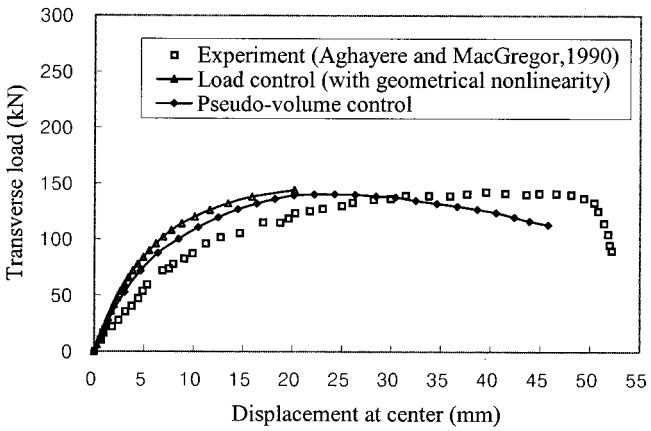

Fig. 10. Response of specimen B1

where $\mathbf{x}=\{x,y,z\}^T$ and $\mathbf{n}$=unit vector normal to the element boundary.

The coordinate of the shell element subject to external load can be updated as

$$\mathbf{x}'=\mathbf{x}+\mathbf{u} \tag{8}$$

where $\mathbf{u}$=displacement vector by associated load. A changed volume can be obtained from Eq. (7) using the updated coordinate. Finally, the pseudovolume of the shell element becomes

$$\Delta V=V'-V=\int_b \mathbf{n}^T\cdot\mathbf{u}\,db=\left(\int_{b^e}\mathbf{n}^T\cdot N\,db^e\right)\mathbf{d}^e \tag{9}$$

where N=shape function (Zienkiewicz and Taylor 1991).

Pressure Node

The pressure node has a single degree of freedom, namely, the uniform change of pressure on the finite shell element, denoted by Δp (Song and Tassoulas 1993). Thus, the shell element in this study has 49 degrees of freedom. The traction increments of shell boundaries are

$$\Delta\mathbf{t}=-\Delta p\mathbf{n} \tag{10}$$

The traction term in the load vector of the finite element method is given by

$$\int_{b^e}N^T(\mathbf{t}+\Delta\mathbf{t})db^e=-(p+\Delta p)\int_{b^e}N^T\mathbf{n}\,db^e \tag{11}$$

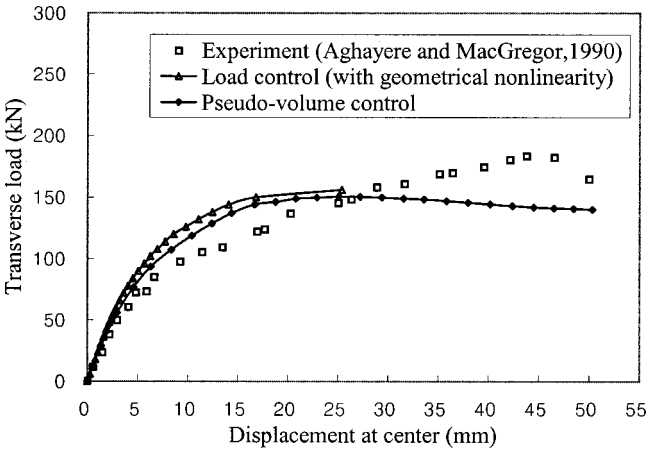

Fig. 11. Response of specimen B2

J. Struct. Eng., 2002, 128(5): 655-664

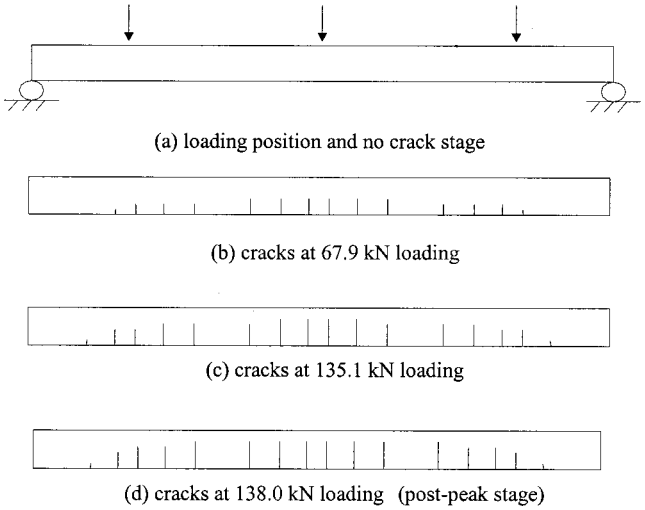

Fig. 12. Centerline crack status of specimen A1 (thickness direction)

Then, the equilibrium equation in the element is given by

$$\mathbf{K}^e\mathbf{d}^e = -(p+\Delta p)\int_{b^e} N^T\mathbf{n}\,db^e + \mathbf{F}^e \tag{12}$$

where $\mathbf{K}^e$ = element stiffness matrix and $\mathbf{F}^e$ = element internal load vector. Absorbing the term involving Δp into the stiffness matrix and inserting Eq. (9), one finds that the element equilibrium equation with matrix form is now given by

$$\begin{bmatrix} \mathbf{K}^e & \displaystyle\int_{b^e} N^T\mathbf{n}\,db^e \\ \displaystyle\int_{b^e} \mathbf{n}^T N\,db^e & 0 \end{bmatrix} \begin{bmatrix} \mathbf{d}^e \\ \Delta p \end{bmatrix} = \begin{bmatrix} -p\displaystyle\int_{b^e} N^T\mathbf{n}\,db^e + \mathbf{F}^e \\ \Delta V \end{bmatrix} \tag{13}$$

where the last row and column in the modified stiffness matrix correspond to the additional degree of freedom Δp, while the load vector now contains the additional component ΔV. The presence of the pseudovolume ΔV in the load vector indicates that

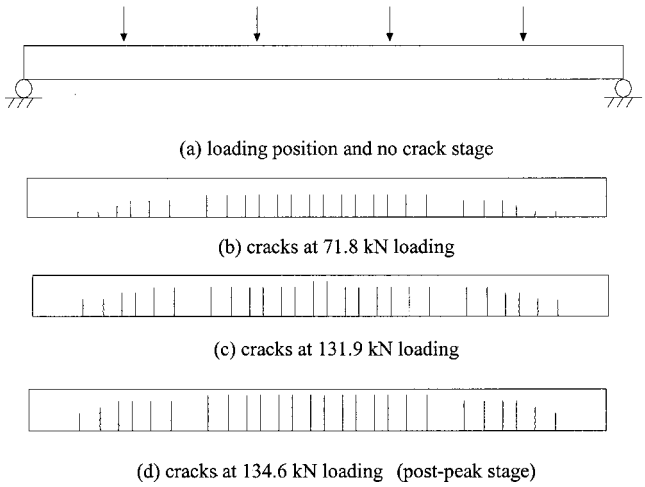

Fig. 13. Centerline crack status of specimen B1 (thickness direction)

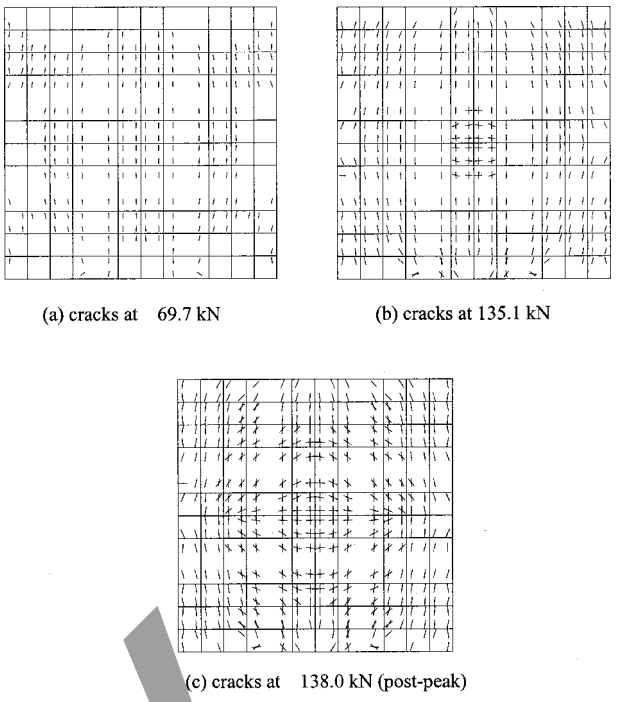

Fig. 14. Crack status at bottom plane of specimen A1 (seventh layer)

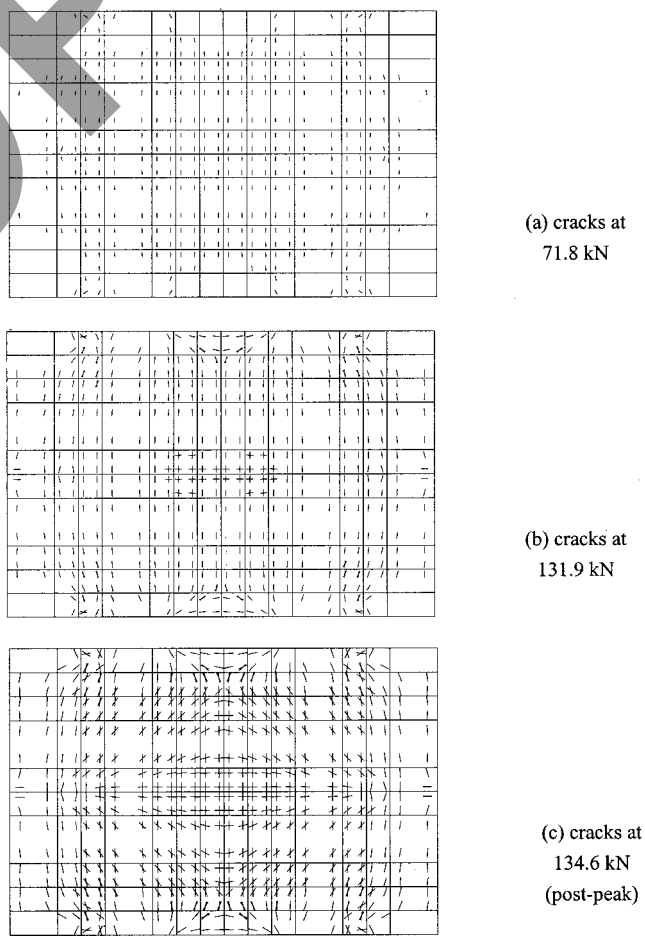

Fig. 15. Crack status at bottom plane of specimen B1 (seventh layer)

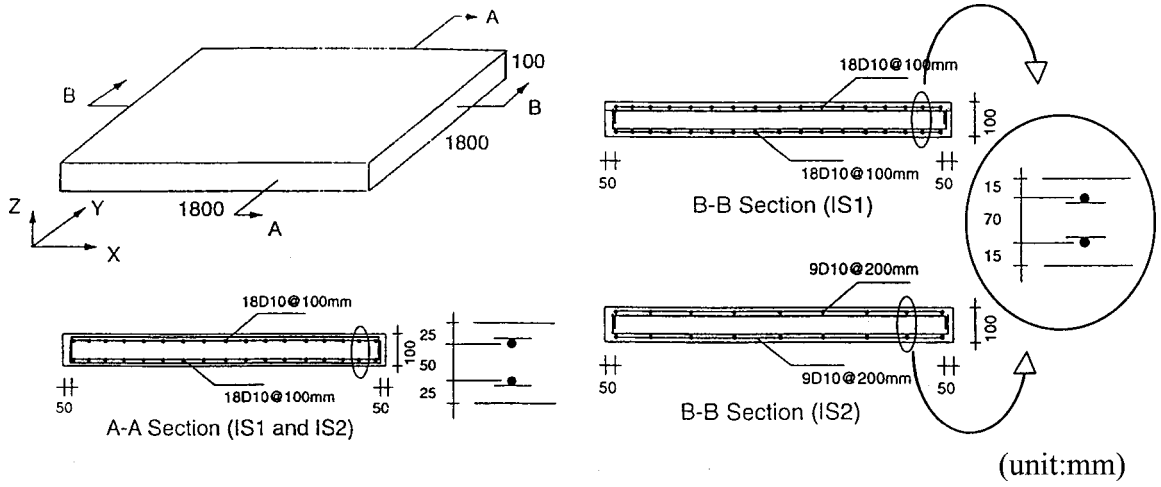

Fig. 16. Detail of slabs (Irawan 1995)

one can specify the change in the pseudovolume of shell structures and determine the required change in pressure. Thus by controlling either continuously increasing or continuously decreasing pseudovolume in nonlinear iterative analysis, one can solve for the required increase or decrease in pressure along equilibrium paths around the ultimate point of pressure. The pseudovolume control iterative procedure of nonlinear analysis is based on the Newton–Raphson method. The iteration can be repeated until pseudovolume equilibrium is reached to the prescribed tolerance. When the volume enclosed by a structure is going to increase or decrease as deformation processes as in snap-through buckling problems, either the pseudovolume control method or the displacement control method cannot be applied and an alternative iterative procedure like the arc-length control method (Crisfield 1981) should be applied.

Failure Analysis of Reinforced Concrete Shell Structures

Slabs Subjected to In-Plane and Out-of-Plane Loads

A series of the University of Alberta's tests on slabs loaded with a combination of in-plane and out-of-plane loadings (Aghayere and MacGregor 1990) was used for the verification of the analysis techniques in this paper. Depending on the aspect ratio, the test slabs were divided into Type-A slabs and Type-B slabs (Figs. 6 and 7). The Type-A slabs are square with dimensions of 1830×1830 mm, while Type-B slabs are rectangular with dimensions of 2744×1830 mm. The thickness of both slabs is approximately 65 mm. The specimens were reinforced with two layers of deformed bars placed in orthogonal directions, with the reinforcement ratios for the top and bottom layers being equal. The specimens were simply supported at certain points around the perimeter as indicated in Figs. 6 and 7. A sequential loading pattern was applied to the slab; in-plane load was first applied to the full magnitude, and kept constant; then, out-of-plane load was applied gradually until the failure of the specimen. In-plane loads were applied along the two sides of the specimens while out-of-plane loads were applied at nine points for the A-type slabs and 12 points for the B-type slabs (Figs. 6 and 7). Details of the specimens and in-plane loads are given in Table 1. For finite element discretization, the A-type slabs were divided into a mesh of 10×10 elements as shown in Fig. 6, while the B-type slabs were divided into a mesh of 7×5 elements as shown in Fig. 7. Note that the symmetry of the slabs was not utilized for the discretization. Along the thickness, seven layers per depth were used. Comparisons of analyses including the effect of geometrical nonlinearity and experiments for specimens A1, A2, B1, and B2 are given in Figs. 8–11.

Table 2. Material Properties of Slab Specimens (Irawan 1995)

Specimen	Concrete properties f'_c (MPa)	Reinforcement ρ_x (%)[a]	ρ_y (%)[a]	f_{sy} (MPa)
IS1	37.0	0.78	0.78	380
IS2	37.0	0.78	0.39	380

[a]Per layer.

Since the thickness of slabs is very small relative to the width of slabs under relatively high in-plane loads, geometrical nonlinearity was significant for these cases. Without the capability to consider the geometrical nonlinearity, the analysis overestimates the capacity of the shell element. It should be noted that the falling branch of the load-deflection curve could not be obtained by analysis of the load control method. However, the pseudovolume control method can predict the load-deflection curve of slabs up to failure including postpeak. Figs. 12 and 13 show crack status occurring at the centerline section of a slab under different vertical loadings for specimen A1 and B1, respectively. They show the propagation of cracks from the bottom layer through thickness. Figs. 14 and 15 also show cracks occurring at the bottom of each slab, i.e., in the seventh layer of each slab; two-way active cracks are activated and radial cracks are developed at postpeak stages, as shown Fig. 14(c). It can be seen that the secondary cracks occur perpendicularly to primary cracks near the center of the slabs, but nonorthogonal secondary cracks to the primary cracks are generated away from the center of the slabs with increase of loading.

Slabs Subjected to Cyclic Transverse Loads

Another series of tests from the University of Tokyo (Irawan 1995) was used for the verification of the technique for the analysis of reinforced concrete slabs subjected to cyclic transverse loads. Two slabs had different arrangements of reinforcing bars

J. Struct. Eng., 2002, 128(5): 655-664

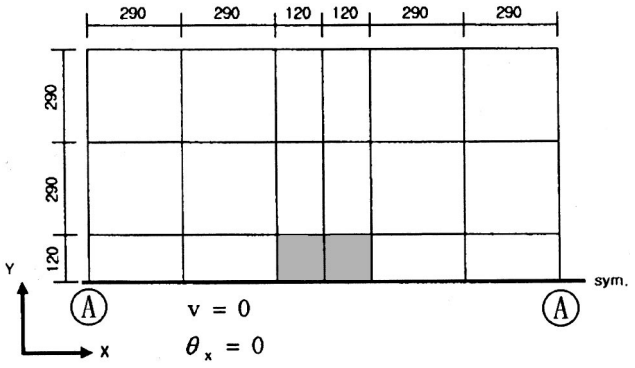

Fig. 17. Element mesh for slab specimen

(isotropic and anisotropic) as shown in Fig. 16; the size of the slab specimens was 1800×1800 mm. In isotropic slab (IS1), the reinforcement ratio in the *x* and *y* directions was equal, while in the anisotropic slab (IS2), the reinforcement ratio in the *x* direction was twice that in the *y* direction. Reinforcement in both specimens was placed in two layers: top and bottom in each of the orthogonal directions. The diameter of the reinforcing bars used in the specimens was 100 mm. The spacing between reinforcing bars was adjusted to obtain a different reinforcement ratio as illustrated in Fig. 16. The material properties of the reinforced concrete slab specimens are given in Table 2. Both slabs were simply supported around the perimeter of the slabs of 1400×1400 mm and transverse cyclic loads were applied at the center of the slab.

In analysis, specimens were modeled using a mesh of 6×3 elements, as shown in Fig. 17, by utilizing the symmetry of the slab in the *y* direction. In Fig. 17, the shadow elements indicate the element where transverse cyclic load applies. Ten layers per element were used for the integration through the depth: from the first layer at the bottom of the slab to the tenth layer at the top of the slab.

Comparisons of results of analyses using the pseudovolume control technique and experimental results for specimens IS1 and IS2 are given Figs. 18 and 19. The analysis can predict the envelope curve of load deflection for both isotropic and anisotropic arrangements of reinforcing bars well. The comparison shows that the analysis also successfully simulates the response of shell structures subjected to cyclic out-of-plane loading except for postpeak prediction, which was not observed in the experiment. However, analysis results show that the technique can be well

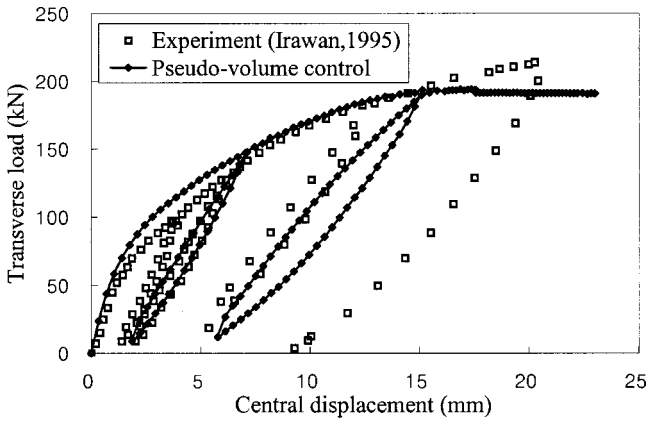

Fig. 18. Behavior of specimen IS1

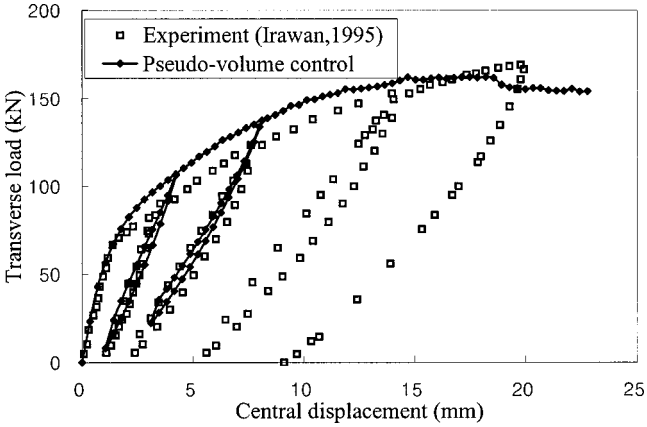

Fig. 19. Behavior of specimen IS2

utilized for the prediction of the quasibrittle, postpeak behavior of a reinforced concrete shell structure. The generation of two-way active cracks at the bottom of isotropic slab IS1 and anisotropic slab IS2 under different loading levels is shown in Figs. 20 and 21, respectively. For cyclic analysis of the shell element, a two-way active crack is observed when the reinforced concrete shell element is subjected to transverse shear accompanying biaxial bending. This indicates that both cracks in the element are opening or closing at the same time in one loading condition. In order to analyze the behavior of a slab subject to cyclic loading, it is noted that the nonorthogonal two-way cracking model was considered in the analysis. Figs. 22(a and b) show the crack propagation through the thickness of each slab.

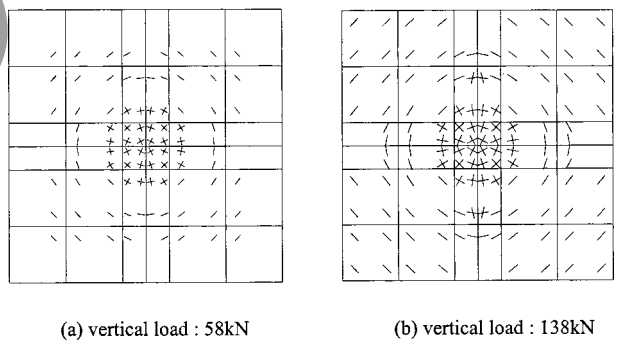

(a) vertical load : 58kN (b) vertical load : 138kN

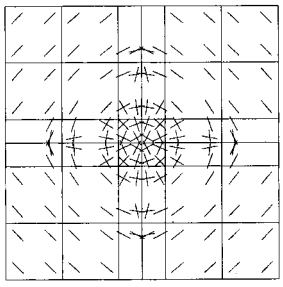

(c) vertical load : 193kN

Fig. 20. Crack status of specimen IS1 (bottom layer)

J. Struct. Eng., 2002, 128(5): 655-664

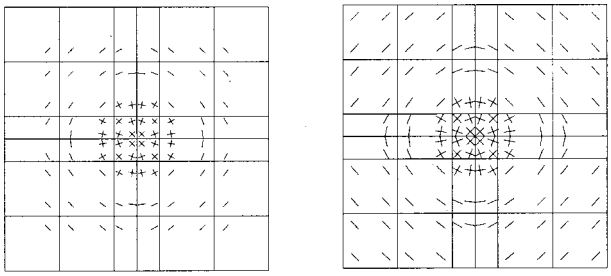

Fig. 21. Crack status of specimen IS2 (bottom layer)

Reinforced Concrete Dome Structure under External Pressures

In order to check the applicability of the pseudovolume control technique in this paper, a RC dome structure designed with three different amounts of reinforcement was analyzed. The material properties of the dome are given in Table 3 for three different reinforcement ratios (Cases A, B and C) including underreinforced design Case C.

In view of the symmetry of the dome shape, only a quarter was modeled for the analysis. All designs were restrained normal translation and tangential rotation around the boundary surface. The geometry and finite element meshes of the RC dome are

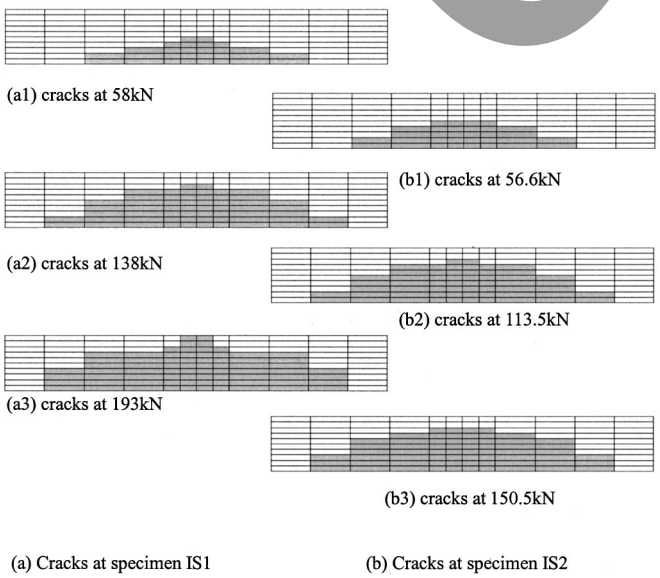

Fig. 22. Crack propagation through thickness

Table 3. Material Properties and Reinforcements of Reinforced Concrete Domes

	Concrete properties		Reinforcement		
Case	f'_c (MPa)	E_c (MPa)	ρ_x (%)[a]	ρ_y (%)[a]	f_{sy} (MPa)
A			2.7	1.8	
B	47.0	33,100	1.5	0.9	459
C			0.5	0.5	

[a]Per layer.

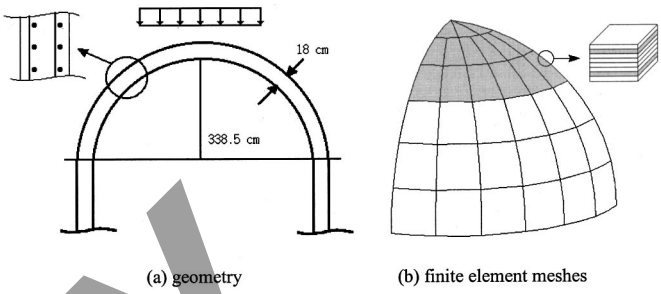

Fig. 23. Geometry and finite element meshes of reinforced concrete dome structure

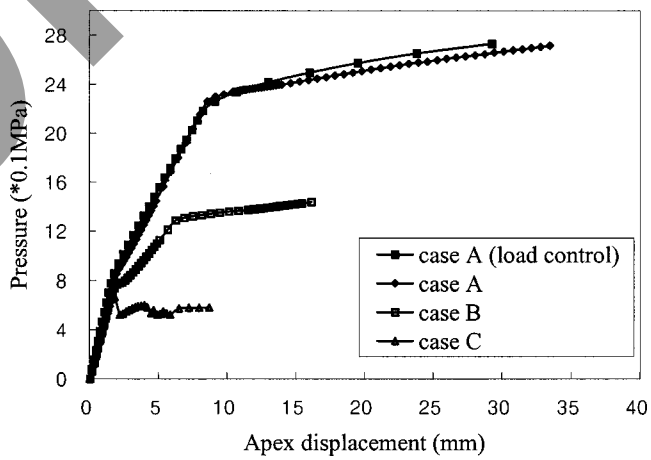

Fig. 24. Response of reinforced concrete domes with different reinforcement ratio

Table 4. Details of Analysis Results for Each Stage (Unit: MPa)

Stage	Case A	Case B	Case C
First cracking	0.62	0.58	0.49
Crack propagation to dome base	0.81	0.74	0.67
Yielding of meridian reinforcement bars	2.30	1.29	No yielding

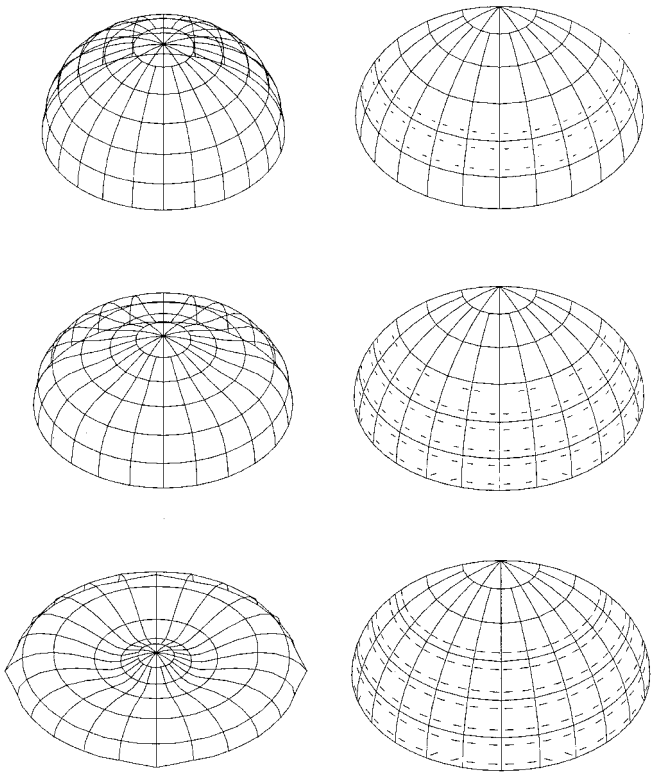

Fig. 25. Deformations and cracks of reinforced concrete dome (Case A)

shown in Fig. 23. As shown in Fig. 23(b), eight layers along the thickness were used for the layered shell element. A concentrated load of 10 kN at dome apex was first applied for initial imperfection and then uniform external pressure was applied only to the shaded elements of dome structure, as shown in Fig. 23.

Predicted responses on apex displacement under uniform external pressure are shown in Fig. 24. For Case A, both the pseudovolume control method and load control method predict well the ductile behavior of the RC dome. However, it should be noted that sudden brittle failure of the underreinforced RC dome is successfully simulated using the volume control method, as shown in Case C in Fig. 24. Detailed analysis results are summarized in Table 4. It is noted that the brittle failure occurs before yielding of the reinforcing bars in Case C. Fig. 25(a) shows 100 times magnified deformations under different uniform external pressures of the RC dome in Case A and Fig. 25(b) shows the propagation-of-crack configuration of the dome in Case A under different external pressures. Meridian cracks occurring at the dome surface about 30° above the dome base propagate down toward the base and up toward the dome apex to about 45° above the base.

Conclusion

In this paper, a failure analysis technique has been developed for the failure analysis of concrete shell structures. Through layered formulation for a layered shell element equipped with a pressure node, path-dependent constitutive models of cracked plain and reinforced concrete were successfully utilized. For the path-dependent crack analysis of RC slabs, geometric nonlinearity and in-plane constitutive equations that can consider crack openings and crack closings according to loading paths are considered by modeling two-way active cracks. By controlling the so-called pseudovolume of shell structures with pressure node formulation, total failure behaviors including the postpeak softening failure behavior of RC shell structures were successfully obtained and verified with experimental data. The ability of the technique to predict the effect of geometrical nonlinearity and postpeak response was verified by using thin slabs subjected to in-plane and out-of-plane loads. The capability of the technique under out-of-plane cyclic load was also verified by predicting reinforced slabs with both isotropic and anisotropic arrangements of reinforcing bars. In order to check the applicability of the technique, failure analysis was carried out for a reinforced concrete dome designed with different reinforcement ratios under uniform external loading. Brittle sudden failure in the case of an underreinforced dome design was successfully simulated using the technique in this paper.

References

Aghayere, A. O., and MacGregor, J. G. (1990). ''Tests of reinforced concrete plates under combined in-plane and transverse loads.'' *ACI Struct. J.*, 87(6), 615–622.

Crisfield, M. A. (1981). ''A fast incremental/iterative solution procedure that handles 'snap-through'.'' *Comput. Struct.*, 13, 55–62.

de Borst, R., and Nauta, P. (1985). ''Non-orthogonal cracks in a smeared finite element model.'' *Eng. Comput.*, 2, 35–46.

Hughes, T. J. R., and Brezzi, F. (1989). ''On drilling degrees-of-freedom.'' *Comput. Methods Appl. Mech. Eng.*, 72, 105–121.

Irawan, P. (1995). ''Three dimensional analysis of reinforced concrete structures.'' PhD dissertation, Univ. of Tokyo, Tokyo.

Kato, B. (1979). ''Mechanical properties of steel under load cycles idealizing seismic action.'' *CEB Bull. Inf.*, 131, 7–27.

Li, B., Maekawa, K., and Okamura, H. (1989). ''Contact density model for stress transfer across cracks in concrete.'' *J. Fac. Eng., Univ. Tokyo (B)* XL(1), 9–52.

Maekawa, K., Irawan, P., and Okamura, H. (1997). ''Path-dependent three-dimensional constitutive laws of reinforced concrete-formulation and experimental verifications.'' *Struct. Eng. Mech.*, 5(6), 743–743.

Maekawa, K., and Okamura, H. (1983). ''The deformational behavior and constitutive equation of concrete using elasto–plastic and fracture model.'' *J. Fac. Eng., Univ. Tokyo (B)* 37(2), 253–328.

Okamura, H., and Maekawa, K. (1991). *Nonlinear analysis and constitutive model in reinforced concrete*, Gihodo-Shuppan, Tokyo.

Polak, M. A. (1992). ''Reinforced concrete shell elements subjected to bending and membrane loads.'' PhD dissertation, Univ. of Toronto, Toronto.

Shima, H., Chou, L., and Okamura, H. (1987). ''Micro and macro models for bond behaviour in reinforced concrete.'' *J. Fac. Eng., Univ. Tokyo (B)*, 39(2), 133–194.

Song, H. W., and Tassoulas, J. L. (1993). ''Finite element analysis of propagating buckles.'' *Int. J. Numer. Methods Eng.*, 36, 3529–3552.

Worsak, K. N. (1979). ''A simple and efficient finite element for general shell analysis.'' *Int. J. Numer. Methods Eng.*, 14, 179–200.

Zienkiewicz, O. C., and Taylor, R. L. (1991). *The finite element method*, Vol. 2, 4th Ed., McGraw-Hill, New York.